Ca^{2+}-binding protein NECAB2 facilitates inflammatory pain hypersensitivity

Ming-Dong Zhang,[1] Jie Su,[1] Csaba Adori,[1] Valentina Cinquina,[2] Katarzyna Malenczyk,[2] Fatima Girach,[2] Changgeng Peng,[3] Patrik Ernfors,[3] Peter Löw,[1] Lotta Borgius,[1] Ole Kiehn,[1] Masahiko Watanabe,[4] Mathias Uhlén,[5] Nicholas Mitsios,[5] Jan Mulder,[5] Tibor Harkany,[1,2] and Tomas Hökfelt[1]

[1]Department of Neuroscience, Karolinska Institutet, Stockholm, Sweden. [2]Department of Molecular Neurosciences, Center for Brain Research, Medical University of Vienna, Vienna, Austria. [3]Division of Molecular Neurobiology, Department of Medical Biochemistry and Biophysics, Karolinska Institutet, Stockholm, Sweden. [4]Hokkaido University School of Medicine, Sapporo, Japan. [5]Science for Life Laboratory, Department of Neuroscience, Karolinska Institutet, Stockholm, Sweden.

Pain signals are transmitted by multisynaptic glutamatergic pathways. Their first synapse between primary nociceptors and excitatory spinal interneurons gates the sensory load. In this pathway, glutamate release is orchestrated by Ca^{2+}-sensor proteins, with N-terminal EF-hand Ca^{2+}-binding protein 2 (NECAB2) being particular abundant. However, neither the importance of NECAB2$^+$ neuronal contingents in dorsal root ganglia (DRGs) and spinal cord nor the function determination by NECAB2 has been defined. A combination of histochemical analyses and single-cell RNA-sequencing showed NECAB2 in small- and medium-sized C- and Aδ D-hair low-threshold mechanoreceptors in DRGs, as well as in protein kinase C γ excitatory spinal interneurons. NECAB2 was downregulated by peripheral nerve injury, leading to the hypothesis that NECAB2 loss of function could limit pain sensation. Indeed, *Necab2*$^{-/-}$ mice reached a pain-free state significantly faster after peripheral inflammation than did WT littermates. Genetic access to transiently activated neurons revealed that a mediodorsal cohort of NECAB2$^+$ neurons mediates inflammatory pain in the mouse spinal dorsal horn. Here, besides dampening excitatory transmission in spinal interneurons, NECAB2 limited pronociceptive brain-derived neurotrophic factor (BDNF) release from sensory afferents. Hoxb8-dependent reinstatement of NECAB2 expression in *Necab2*$^{-/-}$ mice then demonstrated that spinal and DRG NECAB2 alone could control inflammation-induced sensory hypersensitivity. Overall, we identify NECAB2 as a critical component of pronociceptive pain signaling, whose inactivation offers substantial pain relief.

Introduction

Acute pain (nociception) is a physiologically relevant sensation aimed at alerting an individual to, and thus limiting, tissue damage upon contact with harmful stimuli. In turn, chronic pain is the consequence of a series of maladaptive responses following tissue or nerve damage (1, 2). Chronic pain is a rising health problem that afflicts approximately 20% of European adults (3), with treatment options still largely limited to opioids and nonsteroidal antiinflammatory drugs (4–6) and has led to an opioid epidemic, given the addictive side effects and escalated regimes of opioid drugs (4, 7). This is despite the studies providing detailed insights into the cellular determinants of both neuropathic and inflammatory pain (8–20) that motivated drug development (21) following Melzack and Wall's introduction of the "gate control theory" of pain (10).

Ca^{2+} signaling regulates neurotransmitter release at every presynapse of the nervous system (22) by priming the soluble *N*-ethylmaleimide-sensitive factor attachment protein receptor (SNARE) machinery to allow the exocytosis of neurotransmitter-laden vesicles. Among SNARE proteins, synaptotagmin 1 binds Ca^{2+} (with its C2 domains) and is thus an essential Ca^{2+} sensor that converts neuronal activity into fast vesicle release (23). N-terminal EF-hand Ca^{2+}-binding proteins 1–3 (NECAB1–3) are highly homologous members of a family of Ca^{2+} sensors that unconventionally contain only a single EF-hand domain for Ca^{2+} binding. NECAB1 interacts with synaptotagomin 1 at its C2A domain, which also binds syntaxin 1 with high affinity, even if only trace amounts of Ca^{2+} are present (24). NECAB1 and NECAB2 are expressed in neurons (hereafter also termed neuronal Ca^{2+}-binding proteins), with particularly notable expression in dorsal root ganglia (DRGs) and mainly excitatory interneurons in the spinal cord (25). NECAB1 and NECAB2 expression patterns are conserved across mammals (25, 26), highlighting the relevance of their study for human pathologies. Single-cell RNA-sequencing (RNA-seq) identified *Necab2* as a marker of thinly myelinated neurons otherwise coexpressing ($^+$) neurotrophin receptor tyrosine kinase 2 (*Ntrk2*) and neurofilament heavy chain (*Nefh*) in mouse DRGs (27, 28). Since *Ntrk2*$^+$ sensory neurons could contribute to the development of neuropathic pain (besides mediating light touch sensation physiologically) (16), an unanswered yet critical question is whether NECAB2 in these sensory neurons is of functional importance. This is particularly relevant for NECAB2, since, unlike NECAB1, it is regulated at the DRG level by peripheral axotomy (25). How-

Authorship note: MDZ and JS contributed equally to this work. T Harkany and T Hökfelt are co–senior authors.

Conflict of interest: The authors have declared that no conflict of interest exists.

Submitted: March 7, 2018; **Accepted:** June 6, 2018.

Reference information: *J Clin Invest*. 2018;128(9):3757–3768.
https://doi.org/10.1172/JCI120913.

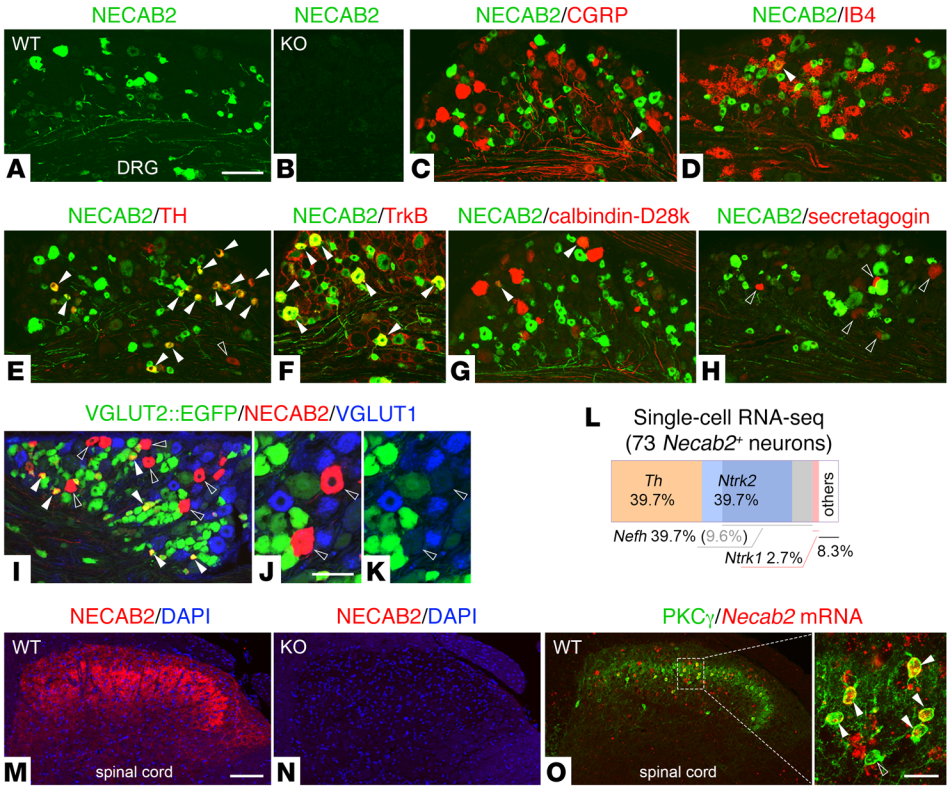

Figure 1. NECAB2 expression in DRGs and spinal cord. (**A** and **B**) NECAB2 immunoreactivity in DRGs from WT and *Necab2*$^{-/-}$ mice showing no residual immunosignal in the mice on a null background (**B**). (**C** and **D**) Coincident detection of NECAB2 and CGRP, a peptidergic marker (**C**), or IB4, a nonpeptidergic marker for nociceptors (**D**). (**E** and **F**) NECAB2 coexists with TH in C-LTMRs (**E**) or TrkB in Aδ D-hair LTMRs (**F**). (**G** and **H**) NECAB2 also colocalized with calbindin D28k (**G**) but not secretagogin (**H**) in DRGs. (**I**) Small-diameter VGLUT2::EGFP, but not VGLUT1$^+$, neurons harbored NECAB2 in DRGs. (**J** and **K**) Neurochemical heterogeneity of NECAB2$^+$ neurons in DRGs. (**L**) Molecular phenotyping of *Necab2*-expressing DRG neurons by reprocessing open-source, single-cell RNA-seq data (26). (**M** and **N**) NECAB2 immunoreactivity in spinal dorsal horn of WT mice (**L**) and its complete loss upon genetic ablation (*Necab2*$^{-/-}$) (**M**). DAPI was used as a nuclear counterstain. (**O**) Colocalization of PKCγ and *Necab2* mRNA in excitatory interneurons in spinal dorsal horn. The rectangle denotes the position of the inset. Projection image for enlarged inset in **O** is from 11-μm-thick tissue samples orthogonally scanned, with optical steps of 1 μm. Tissues from 2 or more mice were processed for histochemical analysis. Solid and open arrowheads point to colocalization and the lack thereof, respectively. Scale bars: 100 μm (**A**–**I** and **M**–**O**), 20 μm (**J**, **K**, and **O**, inset).

ever, it is unclear whether the plasticity of NECAB2 in response to peripheral nerve injury indicates molecular adaptation or affords causality by reducing pronociceptive neurotransmission.

Here, we sought to address the role of NECAB2 in pain circuits at the DRG and spinal levels by combining models for neuropathic and inflammatory pain, behavioral phenotyping, and circuit reconstruction by histochemistry, biochemistry, and genetic access to pain-activated neurons in *Necab2*$^{-/-}$ and WT mice. Our analysis revealed that NECAB2 marks C- and Aδ D-hair low-threshold mechanoreceptors (LTMRs) and excitatory protein kinase Cγ$^+$ (PKCγ$^+$) spinal interneurons. We also show that NECAB2 loss of function (*Necab2*$^{-/-}$) in glutamatergic (excitatory) pathways facilitates behavioral recovery, in large part by decreasing the production and release of brain-derived neurotrophic factor (BDNF) and proinflammatory cytokines upon inflammation. Conversely, genetic rescue of *Necab2* at the spinal level was sufficient to reinstate WT-like pain sensitivity, designating NECAB2 as a critical molecular determinant of pronociceptive neurotransmission.

Results

NECAB2 localization in DRGs and spinal cord. We sought precise information on the localization of NECAB2 in DRGs and spinal cord by combining high-resolution histochemistry and single-cell RNA-seq. First, we applied a high-sensitivity antibody against NECAB2 (HPA014144) to show that 33% ± 2% of DRG neurons, mainly small- and medium-sized ones, express this Ca^{2+}-sensing protein (Figure 1, A and B). These neurons were neither peptidergic (4% ± 1% colocalization with calcitonin gene–related peptide [CGRP]) nor nonpeptidergic (4% ± 2%, iso-lectin B4$^+$ [IB4]) (Figure 1, C and D). Likewise, NECAB2 showed complementarity with calbindin D28k (barring a few exceptions, Figure 1G) and secretagogin (Figure 1H), which are respective Ca^{2+}-binding and alternative Ca^{2+} sensor proteins expressed in DRGs (29). Next, we asked whether NECAB2$^+$ sensory neurons harbor the capacity to produce fast neurotransmitters instead: indeed, these cells were often tyrosine hydroxylase$^+$ (TH$^+$) (Figure 1, E and L) or neurotrophin receptor tyrosine kinase B$^+$ (TrkB$^+$) (Figure 1, F and L), which, by combined single-cell RNA-seq (Figure 1L) and function determination (27), qualifies them as C-LTMRs and Aδ D-hair LTMRs, respectively. Moreover, single-cell RNA-seq validated the likelihood of *Th* and *Vglut2* (the latter encoding vesicular glutamate transporter 2) coexistence (108 *Th*$^+$ cells also contained *Vglut2* mRNA in a pool of 344 *Vglut2*-expressing neurons), reinforcing the idea of an association of NECAB2 with excitatory neurotransmission. In fact, small-sized NECAB2$^+$ neurons were VGLUT2$^+$, whereas we could not detect either VGLUT2- or VGLUT1-like immunoreactivity (LI) in medium-sized neurons (Figure 1, I–K). Finally, we combined ISH and IHC in *Necab2*$^{-/-}$ and WT mice to localize *Necab2* mRNA in PKCγ$^+$ excitatory interneurons in the spinal dorsal horn (Figure 1, M–O). Cumulatively, we believe our findings significantly extend the available data (25, 30) on the association of NECAB2 with excitatory circuits at the DRG and spinal levels.

Peripheral injury downregulates NECAB2 expression in sensory neurons. Upon transecting the sciatic nerve (axotomy), the number of NECAB2$^+$ DRG neurons in lumbar regions 4–6 (always used unless stated otherwise) decreased rapidly and persistently (Figure 2, A–C) and were significantly different from the number detected on the contralateral side 72 hours after injury (34% ± 4%

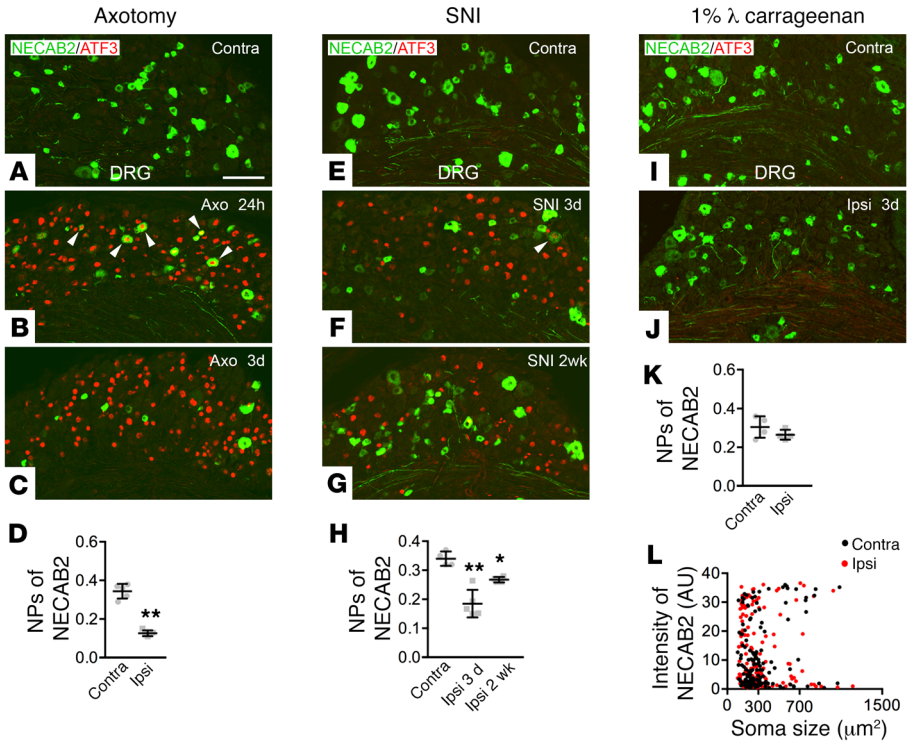

Figure 2. NECAB2 expression in DRGs and spinal cord after peripheral nerve injury and inflammation. (**A**–**D**) Double labeling of NECAB2 and ATF3 in DRGs 24 hours (**B**) and 3 days (**C**) after axotomy (Axo) of the sciatic nerve (n = 5 mice/time point) and quantification of NPs for NECAB2 three days after axotomy. $^{**}P < 0.01$, by Student's t test. (**E**–**H**) Simultaneous detection and subsequent quantification (**H**) of NECAB2 and ATF3 in DRGs 3 days and 2 weeks after SNI (n = 5 mice/time point) revealed significant loss of neuronal immunoreactivity for NECAB2, ipsilateral (Ipsi) to the injury relative to the contralateral (Contra) side. $^{*}P < 0.05$ and $^{**}P < 0.01$, by 1-way ANOVA. (**I**–**K**) Double labeling for NECAB2 and ATF3 in DRGs 3 days after inflammation (1% λ carrageenan) and subsequent quantification of NPs for NECAB2 (n = 4 mice/group). (**L**) Scatter plot of soma size versus relative fluorescence intensity for NECAB2$^+$ DRG neurons 3 days after inflammation. The number of NPs is expressed as a percentage of the total number of neurons (propidium iodide [PI$^+$]) in DRGs throughout. Data are expressed as the mean ± SD. Scale bar: 100 μm (**A**–**C**, **E**–**G**, **I**, and **J**).

[contralateral] vs. 13% ± 1% [ipsilateral], $P < 0.01$; Figure 2D). Ipsilateral to the injury, NECAB2$^+$ neurons frequently and transiently (at 24 h but not 72 h; Figure 2, B and C) coexpressed activating transcription factor 3 (ATF3), a nerve injury marker (31).

We then tested whether spared nerve injury (SNI), a form of neuropathic pain induction that allows functional analysis (32), affects NECAB2 expression. Indeed, we found that *Necab2* mRNA levels were significantly reduced in DRGs, but not spinal cord, ipsilateral to the SNI as compared with the contralateral side, which served as a negative control (1.02 ± 0.22 [contralateral] vs. 0.67 ± 0.16 [ipsilateral], $P < 0.05$ for DRGs; Supplemental Figure 1A). SNI also reduced NECAB2 protein levels as detected histochemically and was quantitatively expressed as a reduced number of NECAB2$^+$ DRG neurons (34% ± 1% [contralateral] vs. 17% ± 5% [ipsilateral, 72 h; $P < 0.01$] or 27% ± 1% [ipsilateral, 2 weeks; $P < 0.05$]; Figure 2, E–H). We found that NECAB2 expression remained unchanged in ipsilateral spinal cord (Supplemental Figure 1, B and C), even though microglia activation (marked by elevated ionized Ca^{2+}–binding adaptor molecule 1 [Iba1]) was seen ipsilaterally in both dorsal and ventral horns, with focal concentration around motor neurons (Supplemental Figure 1D). As with axotomy, NECAB2$^+$ sensory neurons transiently expressed ATF3 after SNI (0.2% ± 0.3% at 72 h, 2% ± 4% after 2 weeks; Figure 2, F and G). In sum, NECAB2 expression was significantly and persistently downregulated in DRG neurons in response to peripheral nerve injury.

Retention of NECAB2 in sensory neurons upon inflammatory pain. Inflammatory pain induced by λ carrageeenan injection into an extremity produces long-lasting hyperalgesia and central sensitization involving, at least in part, C- and Aδ D-hair LTMRs (33). Despite this circuit postulate, we found that λ carrageeenan infusion into a hind paw affected neither the percentage and distribution nor ATF3 expression of NECAB2$^+$ sensory neurons (30% ± 5% [contralateral] vs. 27% ± 3% [ipsilateral]; Figure 2, I–L), even though *Necab2* mRNA was notably downregulated in DRGs (1.00 ± 0.08 [contralateral] to 0.80 ± 0.12 [ipsilateral], P = 0.032) 72 hours after induction (Supplemental Figure 1E). Likewise, neither *Necab2* mRNA nor NECAB2 protein levels were altered in spinal cord after inflammation (Supplemental Figure 1, E and F). Thus, data from injury and inflammatory models suggest that NECAB2 expression is differentially regulated. This finding raises the possibility that NECAB2 might modulate slow-onset and persistent inflammatory pain while undergoing adaptive downregulation, like Ca^{2+}/calmodulin-dependent protein kinase type IV (34), upon irreversible physical injury. This hypothesis also suggests a differential responsiveness of *Necab2*$^{-/-}$ mice to neuropathic versus inflammatory pain.

NECAB1 does not compensate for NECAB2 in Necab2$^{-/-}$ *mice.* We next sought to address NECAB2 function in pain circuits by generating *Necab2*$^{-/-}$ mice with the promoter-driven, KO-first strategy (Figure 3A and ref. 35). By using *Necab2*$^{-/-}$ tissues, we first reevaluated the specificity of the anti-NECAB2 antibodies available to us: HPA013998, used in our previous study (25), showed residual immunoreactivity in DRGs but not spinal cord of *Necab2*$^{-/-}$ mice (Figure 3B), raising the possibility of its unwanted cross-reactivity with NECAB1 (Figure 3C and see the section *Characterization of anti-NECAB2 antibodies* in the Supplemental Information). This is plausible, even if both the HPA013998 and HPA14144 antibodies labeled bands at the calculated molecular weight of NECAB2 in Western blotting (Figure 3D). Notably, an antibody against another Ca2+-sensor protein, secretagogin, also showed similar pattern of specificity with immunolocalization being specific in DRGs but not in spinal superficial layers (see the section *Characterization of anti-secretagogin antibodies* in the Supplemental Information). These observations indicate that an antibody may show correct staining in one tissue but not another and highlight the impor-

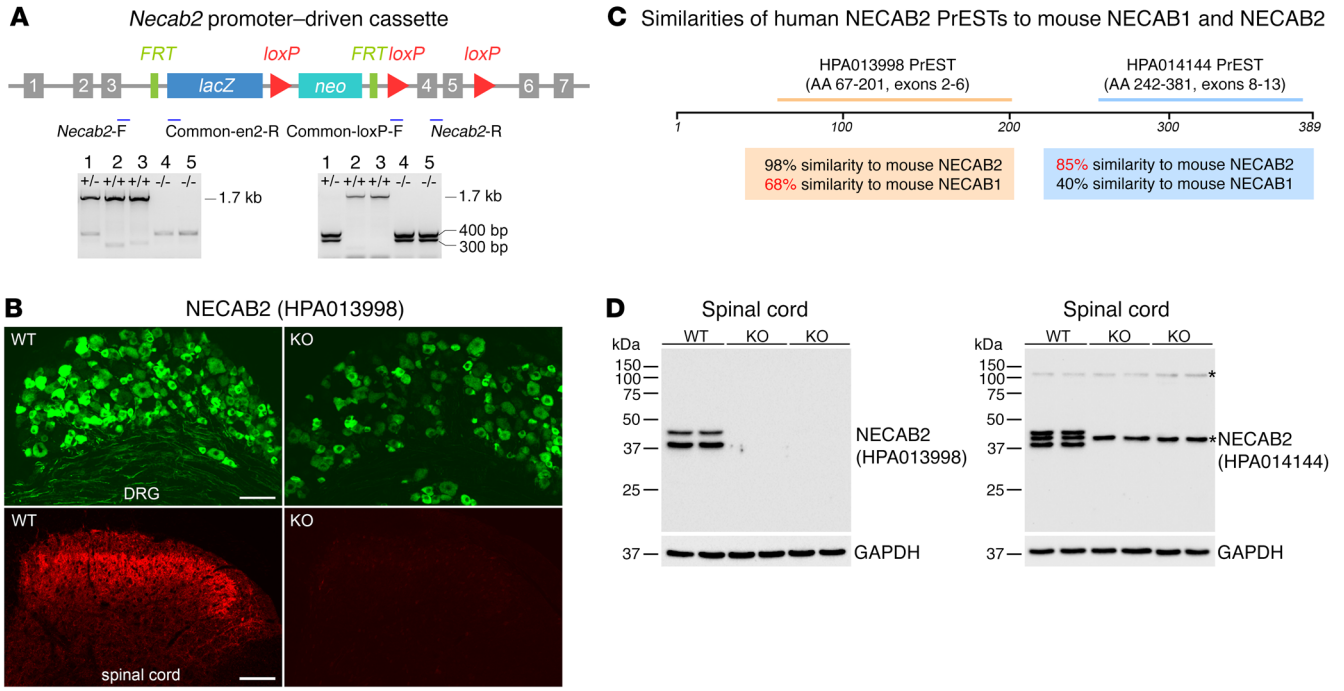

Figure 3. Generation of *Necab2*$^{-/-}$ mice and antibody validation. (**A**) Construct for KO-first, promoter-driven *Necab2*$^{-/-}$ [*Necab2*(tm1a)] mice. The primers (blue lines indicate locations) used for genotyping are shown together with PCR products from WT (lanes 2 and 3), heterozygous (lane 1), and *Necab2*$^{-/-}$ (lanes 4 and 5) offspring. F, forward; R, reverse. (**B**) Staining pattern of previously used anti-NECAB2 antibody (HPA013998) in DRGs (green) and spinal cord (red) from WT and *Necab2*$^{-/-}$ mice. Scale bar: 100 μm. (**C**) Comparison of human NECAB2 protein epitope signature tags (PrESTs) with murine NECAB1 and NECAB2. (**D**) Western blots of NECAB2 with spinal cord lysates from WT and *Necab2*$^{-/-}$ mice using HPA013998 and HPA014144 anti-NECAB2 antibodies. Note that antibody HPA014144 has an unspecific band (asterisk) between 2 specific bands. Representative data from 2 WT and 4 *Necab2*$^{-/-}$ mice are shown. Another nonspecific band occurred above 100 kDa and is also indicated with an asterisk.

tance of testing antibody specificity for each tissue, organ, or system analyzed in KO mice (36, 37).

NECAB proteins exist in 3 isoforms (NECAB1–3), with NECAB1 being the alternative transcript chiefly expressed in the nervous system (23). Therefore, it is plausible that the loss of a NECAB isoform is compensated by another biasing functional phenotype. Here, we show that even though *Necab2*$^{-/-}$ mice have elevated levels of *Necab1* mRNA in both DRGs and spinal cord (Supplemental Figure 2A), this does not translate into increased levels of NECAB1 protein in either structure (Supplemental Figure 2, B–G). We then considered that *Necab2* ablation might modulate VGLUT1–3 expression for glutamate neurotransmission. *Vglut1* mRNA levels in DRGs but not spinal cord (Supplemental Figure 2H) were significantly increased in *Necab2*$^{-/-}$ mice. Consequently, we detected significantly increased protein levels of VGLUT1, which is transported centrally from DRG neurons (38), in *Necab2*$^{-/-}$ spinal cord (Supplemental Figure 2I). *Vglut2* mRNA levels were also elevated in both DRG and spinal cord samples from *Necab2*$^{-/-}$ mice (Supplemental Figure 2H), yet this did not translate into an appreciable increase in the ensuing VGLUT2 protein levels (Supplemental Figure 2J). *Vglut3* mRNA levels remained unchanged in the mice on a *Necab2*$^{-/-}$ background (Supplemental Figure 2H). Likewise, PKCγ and glutamic acid decarboxylase 65 and –67 (GAD65 and GAD67) protein concentrations remained unchanged in *Necab2*$^{-/-}$ mice as compared with concentrations in WT littermates (Supplemental Figure 2, K and L). These data justify the analysis of excitatory (pronociceptive) pain circuits in *Necab2*$^{-/-}$ mice, given that functional recovery could be viewed as counteracting the enhanced glutamatergic neurotransmission.

Necab2$^{-/-}$ *and Scgn*$^{-/-}$ *mice are sensitive to neuropathic pain.* Acute pain sensation (noxious, mechanical stimulus by pinprick) was intact in *Necab2*$^{-/-}$ mice, with no difference between the sexes (Figure 4A). After SNI, *Necab2*$^{-/-}$ mice also developed tactile allodynia (measured by von Frey filament), mechanical hypersensitivity (pinprick), and cold allodynia (acetone) to an extent equivalent to that seen in WT littermates (Figure 4, B–D). We were not able to detect differences between the sexes in the SNI model either. We then analyzed secretagogin-null (*Scgn*$^{-/-}$) mice to determine whether an alternative Ca^{2+} sensor protein (39) also expressed in DRGs (29) would differentially modulate nociception upon neuropathic pain. As with the *Necab2*$^{-/-}$ mice, the *Scgn*$^{-/-}$ animals developed tactile and cold allodynia as well as mechanical hypersensitivity in the SNI model (Figure 4, J–L). Thus, neither Ca^{2+} sensor protein gated nociceptive information transfer from DRGs to ascending centers.

Improved behavioral recovery of Necab2$^{-/-}$ *but not Scgn*$^{-/-}$ *mice after inflammatory pain.* Once we induced inflammation with λ carrageenan, the severity and time course of the development of edema did not differ between *Necab2*$^{-/-}$ and WT mice (Figure 4E), with edema being pronounced by 6 hours, peaking between 24 and 72 hours, and partially receding by day 7 ($P < 0.05$ for the ipsilateral vs. contralateral paw for each time point over the period of 24 hours to 7 days). Tactile allodynia elicited by acute inflammatory pain was

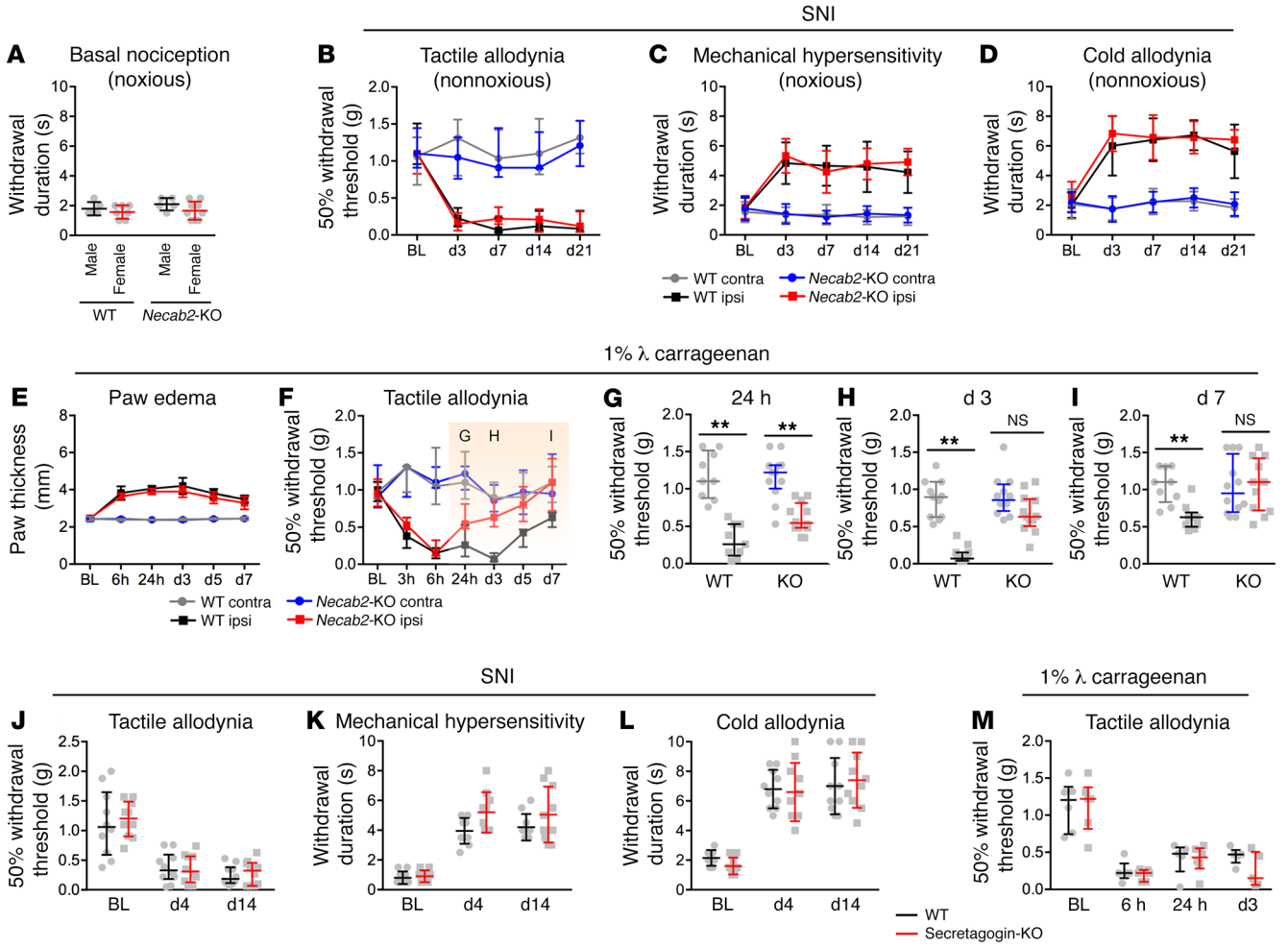

Figure 4. Genetic deletion of NECAB2 gates inflammatory but not neuropathic pain. (**A**) Basal nociceptive sensation (upon noxious mechanical stimulus by pinprick) in *Necab2*$^{-/-}$ mice was intact (relative to WT mice) in a sex-independent manner (n = 5–9/group). (**B**–**D**) After SNI, *Necab2*$^{-/-}$ mice developed tactile allodynia (von Frey filaments, innocuous stimulus), mechanical hypersensitivity (noxious mechanical stimulus), and cold allodynia (acetone stimulus) to a degree equivalent to that of their WT counterparts (n = 12 for WT and n = 14 for *Necab2*$^{-/-}$ mice of both sexes). (**E**) Time course of edema in the hind paw, the typical symptom of inflammation, for WT and *Necab2*$^{-/-}$ mice (n >8/time point/group) after intraplantar injection of λ carrageenan (1%, 20 μl). (**F**) Time course of tactile allodynia after λ carrageenan application differed between *Necab2*$^{-/-}$ and WT mice. (**G**–**I**)Differential responses with the von Frey filament test after inflammation. Note the rapid behavioral recovery upon *Necab2* deletion. (**J**–**L**) After SNI, secretagogin-null (*Scgn*$^{-/-}$) mice (all male) developed tactile allodynia, mechanical hypersensitivity, and cold allodynia that were indistinguishable from what was observed in the WT littermates (n = 10/group). (**M**) Likewise, *Scgn*$^{-/-}$ and WT mice developed tactile allodynia to a similar degree upon λ carrageenan–induced inflammation (n = 6/group). Error bars in black and red correspond to WT and *Scgn*$^{-/-}$ mice, respectively. Behavioral data lacking normal distribution are presented as the median ± interquartile range and were statistically assessed by Mann-Whitney U test (e.g., von Frey filament test). Results of other behavioral assays (e.g., pinprick and acetone stimuli) are expressed as the mean ± SD and were statistically evaluated using a Student's t test (**P < 0.01). BL, basal level.

augmented to a similar degree in *Necab2*$^{-/-}$ and WT mice out to 6 hours (Figure 4F). Yet, inflammatory pain in *Necab2*$^{-/-}$ mice was significantly attenuated by 24 hours (Figure 4G; P = 0.014, ipsilateral paw, *Necab2*$^{-/-}$ vs. WT mice) and reached the basal threshold by 72 hours (Figure 4, H and I). Considering that the extent of edema did not differ between the genotypes studied, we infer that reduced pronociceptive and excitatory signaling at the DRG and spinal levels might facilitate behavioral recovery during the pain consolidation phase in *Necab2*$^{-/-}$ mice. Subsequently, we asked whether this phenotype was specific to NECAB2 or could also be a prototypic response to limiting Ca^{2+} sensor functionality. As such, we found that tactile allodynia after λ carrageenan–induced inflammatory pain in *Scgn*$^{-/-}$ mice was of the same magnitude as that seen in WT controls (Figure 4M). Thus, and in contrast to NECAB2, secretagogin does not appear to molecularly gate pronociceptive excitation associated with inflammatory pain. Moreover, our findings delineate superficial dorsal laminae, in which DRG afferents terminate and innervate (also) NECAB2^{+} excitatory interneurons, as a focus of NECAB2-dependent signaling events.

Convergence of inflammatory signals in spinal cord. We gained insights into the extent of the neuronal circuitry that underpins inflammatory pain signaling by using a genetic reporter approach exploiting permanent genetic access to transiently active neurons, also termed targeted recombination in active (cell) populations (TRAP) (40), driven by the immediate-early gene *Arc*. We focused on recombination events at the spinal level, since *Arc* (alike *Fos*, the

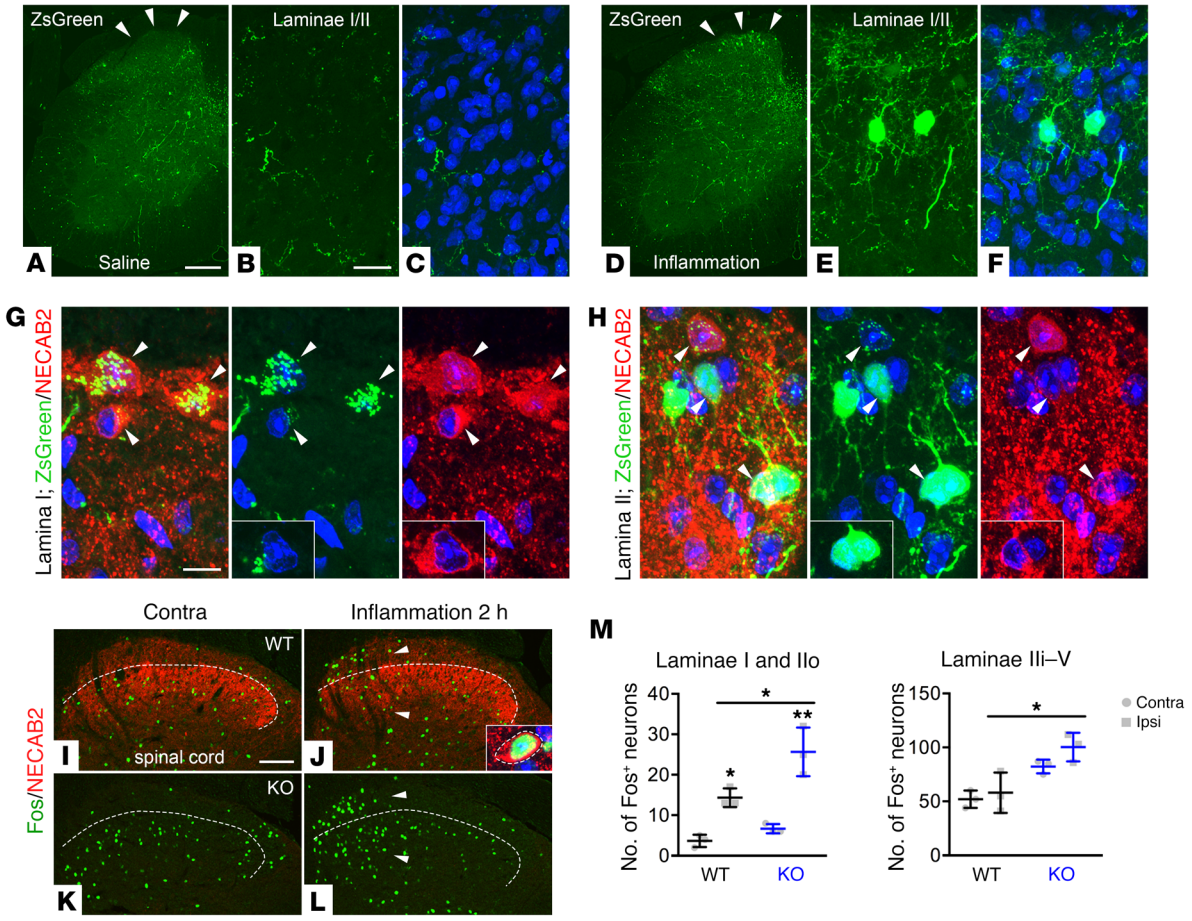

Figure 5. Genetic dissection of spinal neuron activity upon inflammatory pain. (**A**–**F**) Distribution of ZsGreen$^+$ cells in spinal superficial layers from *Arc-CreERT2::Rosa26-stop-ZsGreen* TRAP mice upon saline or λ carrageenan infusion. Tamoxifen was administered for 3 consecutive days after stimulation. PI was used as a nuclear counterstain. Arrowheads in **A** and **D** pinpoint the location of ZsGreen$^+$ neurons in medial spinal superficial layers. (**G** and **H**) High-resolution analysis of ZsGreen showed that these cells were NECAB2$^+$ (arrowheads) in laminae I and II. PI was used as a nuclear counterstain. Projection images rendered from 9- and 12-μm orthogonal stacks in **G** and **H**, respectively, are shown. Insets are single-plane images selected from each deck. (**I**–**L**) Fos$^+$ cells in spinal dorsal horn 2 hours after λ carrageenan stimulation of WT and *Necab2*$^{-/-}$ (KO) mice. Dashed lines label the border between the outer (IIo) and inner (IIi) layers of lamina II. Arrowheads indicate the medial superficial dorsal horn and laminae III and IV. Inset confirms colocalization of Fos and NECAB2. (**M**) Quantification of Fos$^+$ neurons per section in medial laminae I and IIo and laminae IIi to V at the level of lumbar segments 4 and 5 (n = 3 animals/group/genotype). *P < 0.05 and **P < 0.01, by 2-way ANOVA with Tukey's post hoc test. Data are expressed as the mean ± SD. Scale bars: 200 μm (**A** and **B**), 100 μm (**I**–**L**), 20 μm (**B**, **C**, **E**, and **F**), and 10 μm (**G** and **H**).

alternative and experimentally amenable immediate-early gene) seems not to be expressed in DRGs (41). Peripheral inflammation–induced activation of primary sensory afferents coincident with tamoxifen priming (within a window of 6 to 12 h after λ carrageenan injection) in *Arc-CreER^{T2}::ROSA26-stop-ZsGreen* reporter mice (Figure 5, A–F, and Supplemental Figure 3, A and B) allowed us to show that NECAB2$^+$ neurons in laminae I and II of the dorsal spinal horn might have received sufficiently strong synaptic inputs to become ZsGreen$^+$ (Figure 5, G and H). Inflammatory pain–induced activation of NECAB2$^+$ spinal neurons was reinforced by the histochemical colocalization of NECAB2 and Fos (Figure 5, I–L). Like *Arc*-driven ZsGreen expression (Figure 5D), we mainly observed Fos immunoreactivity in medial superficial layers of the spinal cord (Figure 5, J and L), with significantly greater abundance detected in *Necab2*$^{-/-}$ compared with WT mice (Figure 5M and Supplemental Figure 3, C and D). Our histochemical data were validated by a gradual increase in spinal *Fos* mRNA content in *Necab2*$^{-/-}$ mice, reaching significance 90 minutes after intervention (Supplemental Figure 3E). These data cumulatively suggest that NECAB2$^+$ spinal interneurons are cellular determinants of inflammatory pain, and their enhanced activation in *Necab2*$^{-/-}$ mice reflects increased intrinsic network activity to compensate for their functional incompetence when NECAB2 is genetically ablated. Because of the unchanged NECAB2 levels in DRGs upon λ carrageenan administration (Figure 2), we suggest that, in turn, NECAB2 is not rate limiting for pronociceptive excitatory neurotransmission in primary DRG projections to superficial spinal laminae.

Reduced proinflammatory cytokine and BDNF responses in Necab2$^{-/-}$ *mice.* Despite the fact that induction of inflammatory pain (for up to 6 h) and paw edema were indistinguishable between *Necab2*$^{-/-}$ and WT mice (Figure 4E), their differential network activation at the spinal level suggests probable differences in the levels of pronociceptive mediators that are produced and/or released in an activity-dependent manner. We first assayed *Tnfa*, *Il6*, and *Il1b*

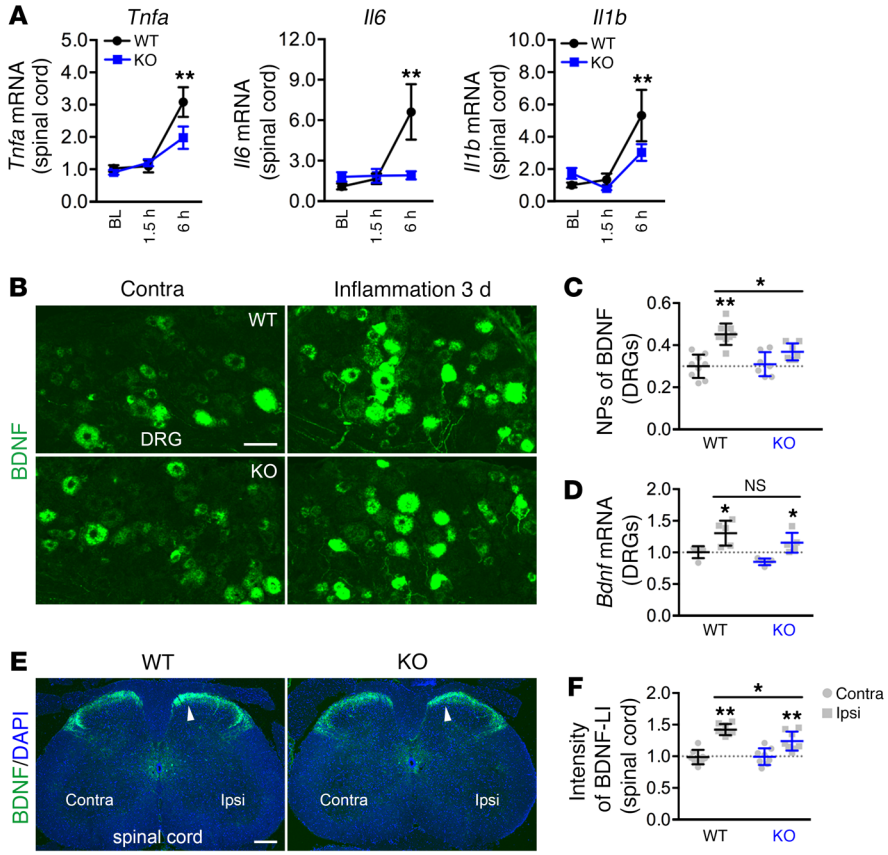

Figure 6. Reduced proinflammatory cytokine and BDNF signaling in *Necab2*$^{-/-}$ mice. (**A**) Inflammation-induced increases in *Tnfa*, *Il6*, and *Il1b* mRNA expression in the spinal cord were diminished by the genetic ablation of *Necab2* (KO) (n = 15 animals/genotype). Two-way ANOVA revealed a significant inflammation genotype interaction [$F_{(2,24)}$ = 5.491, P = 0.0109] for *Il6* after 6 hours of inflammation. $^{**}P < 0.01$, by 2-way ANOVA with Tukey's post hoc test. (**B**) BDNF-like immunoreactivity in DRGs from WT and *Necab2*$^{-/-}$ (KO) mice after 3 days of inflammation. (**C**) Quantification of BDNF$^+$ NPs in DRGs (n = 5 animals/genotype). Two-way ANOVA revealed a significant inflammation genotype interaction [$F_{(2,28)}$ = 6.460, P = 0.0169], with group-wise comparisons returning a significant reaction for WT DRGs. $^*P < 0.05$ and $^{**}P < 0.01$, contralateral vs. ipsilateral, by 2-way ANOVA with Tukey's post hoc test. (**D**) *Bdnf* mRNA in DRGs. Note the similar responses in the *Necab2*$^{-/-}$ mice. (**E** and **F**) BDNF-like immunoreactivity in spinal cord after 3 days of inflammation (**E**) and its quantitative analysis (**F**). Arrowheads in **E** indicate the medial spinal cord superficial layers ipsilaterally. (**F**) Two-way ANOVA revealed a significant inflammation genotype interaction [$F_{(1,28)}$ = 4.694, P = 0.0389]. n = 9 for WT and n = 8 for *Necab2*$^{-/-}$ mice. $^*P < 0.05$ and $^{**}P < 0.01$ by 2-way ANOVA with Tukey's post hoc test. Data are expressed as the mean ± SD. Scale bars: 200 μm (**E**), 50 μm (**B**).

mRNAs (Figure 6A) and found that their transcriptional activation was significantly reduced in *Necab2*$^{-/-}$ mice relative to WT controls. These data concur with glial activation in neuropathic and inflammatory pain models (refs. 42–44 and Supplemental Figure 1D). Next, we histochemically tested whether the expression of BDNF, a neuronal pronociceptive sensitizing factor acting through TrkB signaling (45), is altered by 72 hours following inflammatory pain induction, when mechanical allodynia was significantly improved in *Necab2*$^{-/-}$ mice (Figure 4F). As such, peripheral inflammation significantly increased the number of BDNF$^+$ neurons in WT DRGs (30% ± 6% [contralateral] vs. 45% ± 5% [ipsilateral], $P < 0.05$; Figure 6, B and C), along with a robust increase in *Bdnf* mRNA transcript levels (Figure 6D). In contrast, an inflammation-induced increase in BDNF$^+$ neurons failed to materialize in *Necab2*$^{-/-}$ mice (31% ± 6% [contralateral] vs. 37% ± 4% [ipsilateral]; Figure 6, B and C), even though *Bdnf* transcription increased (Figure 6D). Notably, these differences were also evident at the spinal level, with *Necab2*$^{-/-}$ mice showing significantly attenuated BDNF immunoreactivity in the ipsilateral dorsal horn as compared with WT mice (Figure 6, E and F), even if a hemispheric difference was evident in both genotypes. Taken together, these data suggest that *Necab2* deletion in DRGs attenuates BDNF production and release into the dorsal spinal horn to limit pronociceptive excitatory signaling in *Necab2*$^{-/-}$ mice and could, at least in part, accelerate functional recovery.

Genetic rescue of NECAB2 expression in spinal cord and DRGs reinstates pain sensitivity. NECAB2 is also expressed in hind-, mid-, and forebrain regions, including in nuclei that tune sensory relay (8, 24). Therefore, we asked whether NECAB2 at the spinal level is sufficient to gate pronociceptive signaling. To this end, we exploited the tissue-restricted expression of *Hoxb8* (46), a member of the *Antp* homeobox gene family. *Hoxb8* is expressed in spinal cord neurons and glia as well as in all DRG neurons, while sparing the brain, apart from the spinal trigeminal nucleus. By crossing the *Necab2*(tm1a) allele (Figure 3A) with *Hoxb8-Flp* mice, we successfully reinstated *Necab2* expression below the cervical spinal segment 4 and in DRGs (Figure 7, A–F). Whole-tissue imaging by light-sheet microscopy after iDISCO$^+$ (immunolabeling-enabled three-dimensional imaging of solvent-cleared organs) processing in combination with histochemistry (47) revealed WT-like expression and correct localization for NECAB2 in dorsal spinal horns (Figure 7, D and F) of *Hoxb8*-Flp::*Necab2*(tm1a) mice. Genetic rescue of *Necab2* expression also reinstated WT-like pain sensitivity: *Hoxb8*-Flp::*Necab2*(tm1a) mice developed tactile allodynia, with partial recovery only 7 days after λ carrageenan stimulation (Figure 7, G and H), matching the profile of the WT littermates. Thus, NECAB2 at the spinal level is sufficient to consolidate persistent inflammatory pain.

Discussion

The present study takes advantage of the combination of high-resolution histochemistry and single-cell RNA-seq (27) to molecularly tie NECAB2 expression in DRGs to C-LTMRs and Aδ D-hair LTMRs. NECAB2 levels decrease in sensory neurons upon peripheral nerve injury, whether axotomy or SNI. The use of SNI is notable, because it allows the determination of functional recovery at high temporal resolution (32) and led us to distinguish roles for

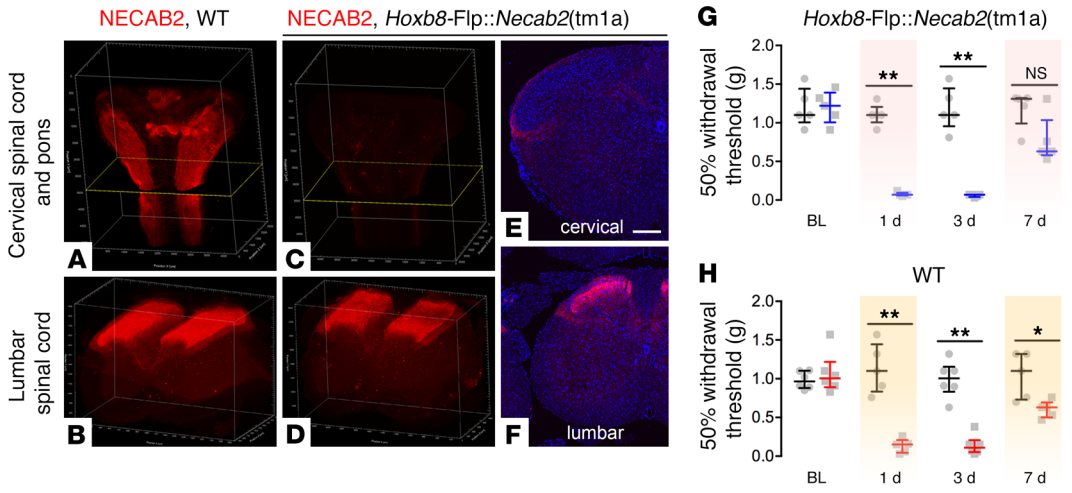

Figure 7. Genetic rescue of *Necab2* at the spinal level reinstates tactile allodynia after inflammation. (**A**–**D**) Graphical rendering of 3D reconstructed intact tissues after NECAB2 IHC using iDISCO⁺ and subsequent light-sheet microscopy. Pons-cervical spinal cord and lumbar spinal cord from WT (**A** and **B**) and *Hoxb8-Flp::Necab2*(tm1a) mice (**C** and **D**) are shown. Note that *Hoxb8* expression is restricted to spinal cord and DRGs. (**E** and **F**) NECAB2 histochemistry in transverse sections of cervical (**E**) and lumbar (**F**) spinal cord from *Hoxb8-Flp::Necab2*(tm1a) mice. Individual planar sections are shown at anatomical coordinates corresponding to **C** and **D**, respectively. Sections were counterstained with DAPI. (**G** and **H**) *Hoxb8-Flp::Necab2*(tm1a) mice (n = 5) developed tactile allodynia after peripheral inflammation (von Frey filament test) to an extent similar to that seen in WT mice (n = 6), even if NECAB2 was not expressed supraspinally. Data are expressed as the median ± interquartile ranges. $^*P < 0.05$ and $^{**}P < 0.01$, by Mann-Whitney U test. Scale bar: 250 μm (**E**).

NECAB2 when combining nerve injury with genetic loss-of-function as well as gain-of-function analyses. Accordingly, NECAB2 is dispensable for the transmission of mechanical but not inflammatory pain. By showing that NECAB2 invariably coexists with VGLUT2 (48) in glutamatergic synapses in primary afferents, excitatory (PKCγ⁺) interneurons, and ascending projections (25), its loss is likely to attenuate excitatory neurotransmission. This is significant, since modulating the excitation-inhibition balance in spinal circuits can alleviate neuropathic pain (49, 50). The involvement of laminae I and II interneurons of the dorsal spinal horn in transmitting inflammation-related nerve activity is reinforced by our immediate early-gene–driven (*Arc*-driven) genetic labeling (TRAP) (40). TRAP marked cells, many being NECAB2⁺, whose activity significantly increased within a 6- to 12-hour time window upon λ carrageenan challenge. When inflicting peripheral inflammation in *Necab2*$^{-/-}$ mice, we observed significant facilitation of post-traumatic recovery that reached basal pain thresholds (that is, a pain-free state) remarkably faster than in WT mice. This finding suggests a pronociceptive "gatekeeper" role for NECAB2, with its action confined to at least 3 levels: (a) intraganglionic signaling between sensory neurons; (b) BDNF (and/or cytokine release, even though we do not exclude the possibility of contribution by glia residing in spinal cord) from nerve endings of primary afferents in the superficial dorsal horn (that is, at the first synapse in the sensory-pain circuit); and (c) dorsal horn interneurons.

Peripheral nerve injury is a stimulus that is sufficiently strong to trigger changes in the expression of hundreds of genes in neurons and glia, which assemble into multimodal pain pathways along DRGs and the spinal cord. The combinatorial outcome of genetic modifications in these pain pathways will underpin pain sensation (e.g., stratify severity), as well as determine the innate capacity for adaptation and regeneration in response to mechanical insults (51–54). We posit that rapid downregulation of NECAB2 could reduce excitation, thus preventing transition to the development of chronic pain. This hypothesis emphasizes a critical role for excitatory spinal interneurons and is molecularly appealing, since NECAB2 is enriched in their VGLUT2⁺ nerve terminals (25), a consensus requirement for all Ca^{2+} sensors regulating the assembly of SNARE complexes for vesicular exocytosis in the presynapse. Besides regulating vesicular docking events, presynaptic signal integration of NECAB2 might involve an interaction with metabotropic glutamate receptor type 5 (mGluR5) (55), which is present in afferents to the dorsal horn (56), where presynaptic mGluR5 receptors enhance glutamate release (57). Thus, *Necab2*$^{-/-}$ mice could have attenuated glutamate release and, consequently, reduced circuit excitation in spinal dorsal horn. Accordingly, genetic or pharmacological dampening of presynaptic NECAB2 availability and/or Ca^{2+} sensitivity in glutamatergic presynapses could protect against excessive pain.

Among the many genes upregulated by synaptic enhancement in laminae I and II are *Arc* and *Fos*, which are rapidly and transiently expressed immediate-early genes. However, neither gene is activated in DRGs (41, 58–60), validating the lack of ZsGreen labeling in TRAP mice upon pain induction (data not shown). Considering that Arc and Fos are reliable markers of spinal neurons (61, 62), our experiments outline a dorsomedial domain in laminae I and II of the dorsal horn, which contains the bulk of the neurons synaptically activated upon inflammatory pain (Figure 5, D and L). Our genetic approach utilized *Arc* activation to mark cellular contingents that respond to inflammatory pain in a binary "yes/no" fashion. Nonetheless, genetic TRAP in this case was insufficient to either correlate Arc and Fos levels and pain-like behaviors or infer the importance of *Fos* as an immediate-early gene for pain sensation (58, 63, 64). In sum, our histochemical and genetic circuit-mapping data cumulatively highlight spinal interneurons whose activation is significantly exacerbated upon

Necab2 deletion. If these are interneurons that reduce circuit excitability, then their activation could attenuate inflammatory pain sensation. Despite the clear dichotomy of *Necab2* involvement in neuropathic versus inflammatory pain, we cannot entirely negate the possibility that upregulation of *Vglut2* in DRGs and spinal cord at the mRNA level upon mechanical stimuli could compensate for and thus phenotypically mask NECAB2 loss of function.

Proinflammatory cytokines, like TNF-α, IL-6, and IL-1β, induce inflammatory pain upon their release from immune cells through local sensitization of nociceptors (43, 65–68). Likewise, such cytokines cause pain when released by glial cells in the spinal cord following peripheral inflammation (44, 69–72). In *Necab2*$^{-/-}$ mice, inflammation-induced spinal expression levels of *Tnfa*, *Il6*, and *Il1b* mRNA were lower than those in WT mice. Even though we did not address the question of whether or how *Necab2* deletion limits microglia activation (and thus neuroinflammation), the translation of cytokine mRNA levels into reduced tissue TNF-α, IL-6, or IL-1β content outlines a candidate mechanism for the attenuation of inflammatory pain. Likewise, λ carrageenan application increased the expression of BDNF, an accepted marker of peripheral inflammation. BDNF is an essential growth factor during nervous system development (73) and modulates synaptic neurotransmission in adults (74). BDNF is expressed by peptidergic nociceptors, stored in large dense-core vesicles (often together with neuropeptides), and released from both A and C fibers in spinal superficial layers (75, 76). BDNF binding to TrkB receptors then triggers central sensitization, including postsynaptic NMDA receptor activation and downstream *Fos* mRNA expression (77–79). Therefore, inhibition of BDNF signaling at the spinal level can reduce progressive (but not acute) inflammatory pain and heat hypersensitivity (45, 80, 81). Our data suggest that both BDNF and NECAB2 are presynaptic determinants of glutamatergic hyperactivity upon persistent pain, with BDNF modulating postsynaptic receptor accessibility and/or hypersensitivity (e.g., NMDA receptors), whereas NECAB2 scales glutamate and BDNF release from excitatory nerve terminals. Here, we show that *Necab2*$^{-/-}$ mice failed to respond to inflammatory stimuli by increasing BDNF in primary afferents in laminae I and II, an observation that defines a DRG-locked mechanism for NECAB2. Consequently, attenuated BDNF (and probably cytokine) signaling in spinal superficial layers of *Necab2*$^{-/-}$ mice can curtail circuit hypersensitivity and thus promote recovery after inflammation. Even though BDNF is primarily associated with excitatory neurotransmission, data exist on glia-derived BDNF production and focal release upon injury (82–85). Therefore, and despite the fact that Iba1^{+} microglia were BDNF^{-} in our WT specimens, we cannot entirely rule out an effect, however indirect, of *Necab2* deletion on attenuated BDNF production in microglia upon peripheral inflammation. In sum, inhibition of coincident occlusion of NECAB2-mediated vesicular glutamate and BDNF exocytosis in excitatory spinal interneurons, BDNF^{+}TrkB^{+}VGLUT2^{+} DRG neurons (77, 86), and perhaps resident microglia could prove particularly efficient in limiting pain signaling brought about by peripheral inflammation. Our assertion is compatible with recent patent literature (87, 88), in which NECAB2 is named as a biomarker and prospective druggable target for rheumatoid arthritis and multiple sclerosis.

There are efficient endogenous mechanisms to defend against persistent pain, particularly with inflammatory origins. In addition to descending systems (89), local dorsal horn neurons expressing opioid peptides suppress pain signaling via their cognate receptor systems (90, 91). Opioid receptors are therefore preferred targets for many analgesic drugs, the most efficient being morphine. Neuropathic pain, which results from a more instantaneous insult, is controlled by modulating DRG sensory neurons through, e.g., the 29-aa-long peptide galanin (92). The present report reconciles the above difference of action by identifying pronociceptive NECAB2 as a molecular determinant of inflammatory pain at the DRG and spinal interneuron levels, with its downregulation being causal for preventing persistent pain and facilitating functional recovery. The presynaptic site of action for NECAB2 is also of benefit to dampen BDNF release directly and antiinflammatory cytokine production indirectly in the spinal cord, thus producing a palette of coordinated actions to reduce the coincident and activity-dependent release of fast neurotransmitters and proinflammatory neuromodulators from DRG afferents and excitatory spinal interneurons. We believe these findings will help address the unmet need for therapies beyond opiates in today's epidemic, particularly since chronic inflammatory pain affects 1.7%–5% of the general population (vs. 8% suffering from chronic neuropathic pain) (9, 93–95).

Methods

Animals. WT male C57BL/6 mice (adult, ~15 weeks of age) were obtained from Charles River Laboratories. *Necab2* and *Scgn* KO-first, promoter-driven mice were custom generated by the Knockout Mouse Project (KOMP) Repository at UC Davis (Davis, California, USA). *Hoxb8-Flp*, *Vglut2*::EGFP, and *Arc-Cre*$^{ERT/2}$::ROSA26-stop-*ZsGreen1* mice were obtained from obtained from Ole Kiehn (Karolinska Institutet) and The Jackson Laboratory (catalog 021881). Animals were kept in standard conditions, including a 12-hour light/12-hour dark cycle with ad libitum access to food and water. Efforts were made to minimize the number of mice used and their suffering throughout the experiments.

Surgery. Complete transection of the sciatic nerve (axotomy) at the mid-thigh level of the hind leg was performed as described previously (96). SNI was performed according to previously published protocols (32, 97). For the carrageenan model, mice received an intraplantar injection of 1% λ carrageenan (in 20 μl volume; Sigma-Aldrich) into the hind paw (28-gauge needle) (98) (see Supplemental Methods).

Tamoxifen-induced TRAP. Tamoxifen was dissolved in corn oil (Sigma-Aldrich) and injected s.c. (150–200 mg/kg; Sigma-Aldrich) into *Arc* TRAP mice 12 hours before 1% λ carrageenan infusion (40, 99). *Arc* TRAP mice (vehicle and carrageenan) were perfused either 6 or 72 hours after the onset of inflammation, with the latter time point being particularly suited to allow increased cellular ZsGreen1 content in activated cell populations. Mice that survived to 72 hours received subsequent tamoxifen doses daily.

Behavioral assessment. The withdrawal threshold was tested in transparent plastic domes on a metal mesh floor and measured according to a logarithmically incremental stiffness of 0.04, 0.07, 0.16, 0.40, 0.60, 1.0, and 2.0 g von Frey filament (Stoelting) combined with an up-down method to assess tactile allodynia (32, 100, 101). For mechanical hyperalgesia, a safety pin was used and the duration of paw withdrawal recorded (32). Cold allodynia was tested with a drop of acetone, and the duration of the withdrawal response was recorded (32).

Quantitative real time-PCR. Total RNA was isolated and extracted using TRI Reagent (Sigma-Aldrich). Quantitative real-time PCR (qPCR)

reactions were performed using Maxima SYBR Green Master Mix with ROX (Thermo Fisher Scientific) on an Applied Biosystems QuantStudio 5 unit. The primer pairs used are listed in Supplemental Table 1.

Western blotting. Total protein samples were extracted from freshly dissected DRGs and spinal cords of WT and *Necab2*-KO mice using radioimmunoprecipitation assay lysis buffer and subjected to Western blotting as described previously (25) (see Supplemental Methods). See complete unedited blots in the supplemental material.

Tissues and IHC. For IHC, mice were deeply anesthetized and transcardially perfused with 4% paraformaldehyde (29) (see Supplemental Methods). The primary antibodies used in this study are listed in Supplemental Table 2.

ISH and IHC. Spinal cord cryosections (20-μm, as above) were processed and hybridized as previously described with minor modifications (102). Digoxigenin-labeled (DIG-labeled) *Necab2* RNA probe was used (26). Subsequently, alkaline-phosphatase–conjugated anti-DIG antibody (goat antibody, 1: 2,000; Roche) was applied and developed with Fast Red (Roche). Post-hybridization immunostaining for PKCγ (rabbit antibody, 1:100) was visualized with Alexa Fluoro 488–conjugated affinity-purified donkey anti-rabbit IgG (1:100; Jackson ImmunoResearch) at 22°C to 24°C for 2 hours. After rinsing, sections were coverslipped with 1,4-diazabicyclo[2.2.2]octane (DABCO) (Sigma-Aldrich).

Microscopy and image processing. Representative images were acquired on a Zeiss LSM700 confocal laser scanning microscope (Carl Zeiss) at 1 airy unit pinhole settings and processed in ZEN2012 (Zeiss). Multi-panel figures were assembled with Adobe Photoshop CS6 (see Supplemental Methods).

Quantitative morphometry. Quantification of neuronal profiles (NPs) in DRGs, fluorescence intensity in DRGs and spinal cord, and size distribution analyses were performed on tile-scanned images captured on a Zeiss LSM700 laser scanning microscope (30) (see Supplemental Methods).

iDISCO⁺ and volume imaging. iDISCO⁺ tissue clearing, immunostaining, and volume imaging were performed as described previously (47) (see Supplemental Methods).

Single-cell RNA-seq. Expression data on DRG neurons were reprocessed using the data set published by Usoskin et al. (27) and are deposited in the NCBI's Gene Expression Omnibus database (GEO GSE59739).

Statistics. Behavioral data (e.g., von Frey filament test) lacking normal distribution are presented as the median ± interquartile range and assessed by the Mann-Whitney *U* test. For pinprick and acetone stimuli, data are expressed as the mean ± SD and evaluated by an unpaired, 2-tailed Student's *t* test using GraphPad Prism 6 (GraphPad Software). Data for qPCR, Western blotting, and IHC are presented as the mean ± SD and were also calculated by 2-tailed Student's *t* test (nerve injury and inflammation models in WT mice) or 2-way ANOVA with Bonferroni's or Tukey's multiple comparisons post hoc analysis where relevant (e.g., genotype on inflammation). A *P* value of less than 0.05 was considered statistically significant.

Study approval. Experiments using laboratory rodents were performed in compliance with Swedish regulations and approved by the Norra Djurförsöksetiska Nämnd (N16/15 and N101/14) regional ethics committee in Stockholm.

Author contributions

MDZ, T Harkany, and T Hökfelt designed experiments. MDZ, JS, CA, VC, and CP performed experiments and analyzed data. KM, FG, PL, LB, OK, MW, MU, NM, and JM developed and provided unique reagents, model systems, and experimental tools. PE, OK, MU, T Harkany, and T Hökfelt procured funding for this work. MDZ, T Harkany, and T Hökfelt wrote the manuscript. All authors commented on and approved the submission of this work.

Acknowledgments

We thank Ingrid Nylander (Uppsala University, Uppsala, Sweden) and Lars Terenius (Karolinska Institutet) for supplying the CGRP antiserum, as well as Natalie Sleiers (Karolinska Institutet) and Tony Jimenez-Beristain (Science for Life Laboratory, Solna, Sweden) for their help with the *Vglut2*::EGFP and *Necab2*$^{-/-}$ colonies. Laser scanning microscopy was made available by the Center for Live Imaging of Cells core at Karolinska Institutet, supported by the Knut and Alice Wallenberg Foundation. Support for this study was provided by the Swedish Medical Research Council (to T Harkany, T Hökfelt, and OK); the Karolinska Institutet partial financing scheme for graduate students (to T Harkany and T Hökfelt); the Novo Nordisk Foundation (to T Harkany and T Hökfelt); the European Research Council (ERC Advanced Grants, to T Harkany and OK); the Swedish Brain Foundation (to T Harkany and T Hökfelt); and the European Commission's 7th Framework Programme "PAINCAGE" integrated grant (to T Harkany and T Hökfelt).

Address correspondence to: Tibor Harkany, Department of Molecular Neurosciences, Center for Brain Research, Medical University of Vienna, Spitalgasse 4, A-1090 Vienna, Austria. Phone: 43.1.40160.34050; Email: tibor.harkany@meduniwien.ac.at. Or to: Tomas Hökfelt, Department of Neuroscience, Retzius väg 8, Karolinska Institutet, SE-17177 Stockholm, Sweden. Phone: 46.8.524.87070; Email: tomas.hokfelt@ki.se.

MDZ and JS's present address is: Division of Molecular Neurobiology, Department of Medical Biochemistry and Biophysics, Karolinska Institutet, Stockholm, Sweden.

1. Woolf CJ. What is this thing called pain? *J Clin Invest*. 2010;120(11):3742–3744.
2. Woolf CJ. Generation of acute pain: central mechanisms. *Br Med Bull*. 1991;47(3):523–533.
3. van Hecke O, Torrance N, Smith BH. Chronic pain epidemiology and its clinical relevance. *Br J Anaesth*. 2013;111(1):13–18.
4. Grosser T, Woolf CJ, FitzGerald GA. Time for nonaddictive relief of pain. *Science*. 2017;355(6329):1026–1027.
5. Dowell D, Haegerich TM, Chou R. CDC Guideline for Prescribing Opioids for Chronic Pain — United States, 2016. *JAMA*. 2016;315(15):1624–1645.
6. Moore RA, Derry S, Simon LS, Emery P. Nonsteroidal anti-inflammatory drugs, gastroprotection, and benefit-risk. *Pain Pract*. 2014;14(4):378–395.
7. Majumdar S, Devi LA. Strategy for making safer opioids bolstered. *Nature*. 2018;553(7688):286–288.
8. Basbaum AI, Bautista DM, Scherrer G, Julius D. Cellular and molecular mechanisms of pain. *Cell*. 2009;139(2):267–284.
9. Ji RR, Xu ZZ, Gao YJ. Emerging targets in neuroinflammation-driven chronic pain. *Nat Rev Drug Discov*. 2014;13(7):533–548.
10. Melzack R, Wall PD. Pain mechanisms: a new theory. *Science*. 1965;150(3699):971–979.
11. Braz J, Solorzano C, Wang X, Basbaum AI. Transmitting pain and itch messages: a contemporary view of the spinal cord circuits that generate gate control. *Neuron*. 2014;82(3):522–536.
12. Woolf CJ, Salter MW. Neuronal plasticity: increasing the gain in pain. *Science*.

2000;288(5472):1765–1769.
13. Julius D, Basbaum AI. Molecular mechanisms of nociception. *Nature*. 2001;413(6852):203–210.
14. Woolf CJ. Evidence for a central component of post-injury pain hypersensitivity. *Nature*. 1983;306(5944):686–688.
15. Hökfelt T, Kellerth JO, Nilsson G, Pernow B. Substance p: localization in the central nervous system and in some primary sensory neurons. *Science*. 1975;190(4217):889–890.
16. Peng C, et al. miR-183 cluster scales mechanical pain sensitivity by regulating basal and neuropathic pain genes. *Science*. 2017;356(6343):1168–1171.
17. Xanthos DN, Sandkühler J. Neurogenic neuroinflammation: inflammatory CNS reactions in response to neuronal activity. *Nat Rev Neurosci*. 2014;15(1):43–53.
18. Scholz J, Woolf CJ. The neuropathic pain triad: neurons, immune cells and glia. *Nat Neurosci*. 2007;10(11):1361–1368.
19. Basbaum AI, Woolf CJ. Pain. *Curr Biol*. 1999;9(12):R429–R431.
20. Bessou P, Perl ER. Response of cutaneous sensory units with unmyelinated fibers to noxious stimuli. *J Neurophysiol*. 1969;32(6):1025–1043.
21. Yekkirala AS, Roberson DP, Bean BP, Woolf CJ. Breaking barriers to novel analgesic drug development. *Nat Rev Drug Discov*. 2017;16(8):545–564.
22. Sudhof TC. The presynaptic active zone. *Neuron*. 2012;75(1):11–25.
23. Sudhof TC. Synaptotagmins: why so many? *J Biol Chem*. 2002;277(10):7629–7632.
24. Sugita S, Ho A, Südhof TC. NECABs: a family of neuronal Ca(2+)-binding proteins with an unusual domain structure and a restricted expression pattern. *Neuroscience*. 2002;112(1):51–63.
25. Zhang MD, et al. Neuronal calcium-binding proteins 1/2 localize to dorsal root ganglia and excitatory spinal neurons and are regulated by nerve injury. *Proc Natl Acad Sci U S A*. 2014;111(12):E1149–E1158.
26. Zhang MD, et al. Comparative anatomical distribution of neuronal calcium-binding protein (NECAB) 1 and -2 in rodent and human spinal cord. *Brain Struct Funct*. 2016;221(7):3803–3823.
27. Usoskin D, et al. Unbiased classification of sensory neuron types by large-scale single-cell RNA sequencing. *Nat Neurosci*. 2015;18(1):145–153.
28. Li CL, et al. Somatosensory neuron types identified by high-coverage single-cell RNA-sequencing and functional heterogeneity. *Cell Res*. 2016;26(1):83–102.
29. Shi TJ, et al. Secretagogin is expressed in sensory CGRP neurons and in spinal cord of mouse and complements other calcium-binding proteins, with a note on rat and human. *Mol Pain*. 2012;8:80.
30. Zhang MD, et al. Orthopedic surgery modulates neuropeptides and BDNF expression at the spinal and hippocampal levels. *Proc Natl Acad Sci U S A*. 2016;113(43):E6686–E6695.
31. Tsujino H, et al. Activating transcription factor 3 (ATF3) induction by axotomy in sensory and motoneurons: A novel neuronal marker of nerve injury. *Mol Cell Neurosci*. 2000;15(2):170–182.
32. Decosterd I, Woolf CJ. Spared nerve injury: an animal model of persistent peripheral neuropathic pain. *Pain*. 2000;87(2):149–158.
33. Francois A, et al. The low-threshold calcium channel Cav3.2 determines low-threshold mechanoreceptor function. *Cell Rep*. 2015;10(3):370–382.
34. Ji RR, et al. Ca^{2+}/calmodulin-dependent protein kinase type IV in dorsal root ganglion: colocalization with peptides, axonal transport and effect of axotomy. *Brain Res*. 1996;721(1-2):167–173.
35. Skarnes WC, et al. A conditional knockout resource for the genome-wide study of mouse gene function. *Nature*. 2011;474(7351):337–342.
36. Uhlen M, et al. A proposal for validation of antibodies. *Nat Methods*. 2016;13(10):823–827.
37. Saper CB. An open letter to our readers on the use of antibodies. *J Comp Neurol*. 2005;493(4):477–478.
38. Brumovsky P, Watanabe M, Hökfelt T. Expression of the vesicular glutamate transporters-1 and -2 in adult mouse dorsal root ganglia and spinal cord and their regulation by nerve injury. *Neuroscience*. 2007;147(2):469–490.
39. Wagner L, et al. Cloning and expression of secretagogin, a novel neuroendocrine- and pancreatic islet of Langerhans-specific Ca^{2+}-binding protein. *J Biol Chem*. 2000;275(32):24740–24751.
40. Guenthner CJ, Miyamichi K, Yang HH, Heller HC, Luo L. Permanent genetic access to transiently active neurons via TRAP: targeted recombination in active populations. *Neuron*. 2013;78(5):773–784.
41. Hunt SP, Pini A, Evan G. Induction of c-fos-like protein in spinal cord neurons following sensory stimulation. *Nature*. 1987;328(6131):632–634.
42. Ji RR, Chamessian A, Zhang YQ. Pain regulation by non-neuronal cells and inflammation. *Science*. 2016;354(6312):572–577.
43. McMahon SB, La Russa F, Bennett DL. Crosstalk between the nociceptive and immune systems in host defence and disease. *Nat Rev Neurosci*. 2015;16(7):389–402.
44. Berta T, et al. Extracellular caspase-6 drives murine inflammatory pain via microglial TNF-α secretion. *J Clin Invest*. 2014;124(3):1173–1186.
45. Mannion RJ, et al. Neurotrophins: peripherally and centrally acting modulators of tactile stimulus-induced inflammatory pain hypersensitivity. *Proc Natl Acad Sci U S A*. 1999;96(16):9385–9390.
46. Witschi R, Johansson T, Morscher G, Scheurer L, Deschamps J, Zeilhofer HU. Hoxb8-Cre mice: A tool for brain-sparing conditional gene deletion. *Genesis*. 2010;48(10):596–602.
47. Renier N, et al. Mapping of brain activity by automated volume analysis of immediate early genes. *Cell*. 2016;165(7):1789–1802.
48. Fremeau RT Jr, et al. The expression of vesicular glutamate transporters defines two classes of excitatory synapse. *Neuron*. 2001;31(2):247–260.
49. Foster E, et al. Targeted ablation, silencing, and activation establish glycinergic dorsal horn neurons as key components of a spinal gate for pain and itch. *Neuron*. 2015;85(6):1289–1304.
50. Bráz JM, et al. Forebrain GABAergic neuron precursors integrate into adult spinal cord and reduce injury-induced neuropathic pain. *Neuron*. 2012;74(4):663–675.
51. Xiao HS, et al. Identification of gene expression profile of dorsal root ganglion in the rat peripheral axotomy model of neuropathic pain. *Proc Natl Acad Sci U S A*. 2002;99(12):8360–8365.
52. Yang L, et al. Peripheral nerve injury induces trans-synaptic modification of channels, receptors and signal pathways in rat dorsal spinal cord. *Eur J Neurosci*. 2004;19(4):871–883.
53. Hökfelt T, Zhang X, Wiesenfeld-Hallin Z. Messenger plasticity in primary sensory neurons following axotomy and its functional implications. *Trends Neurosci*. 1994;17(1):22–30.
54. Costigan M, et al. Replicate high-density rat genome oligonucleotide microarrays reveal hundreds of regulated genes in the dorsal root ganglion after peripheral nerve injury. *BMC Neurosci*. 2002;3:16.
55. Canela L, et al. The association of metabotropic glutamate receptor type 5 with the neuronal Ca^{2+}-binding protein 2 modulates receptor function. *J Neurochem*. 2009;111(2):555–567.
56. Jia H, Rustioni A, Valtschanoff JG. Metabotropic glutamate receptors in superficial laminae of the rat dorsal horn. *J Comp Neurol*. 1999;410(4):627–642.
57. Park YK, Galik J, Ryu PD, Randic M. Activation of presynaptic group I metabotropic glutamate receptors enhances glutamate release in the rat spinal cord substantia gelatinosa. *Neurosci Lett*. 2004;361(1–3):220–224.
58. Harris JA. Using c-fos as a neural marker of pain. *Brain Res Bull*. 1998;45(1):1–8.
59. Jasmin L, Gogas KR, Ahlgren SC, Levine JD, Basbaum AI. Walking evokes a distinctive pattern of Fos-like immunoreactivity in the caudal brainstem and spinal cord of the rat. *Neuroscience*. 1994;58(2):275–286.
60. Menétrey D, Gannon A, Levine JD, Basbaum AI. Expression of c-fos protein in interneurons and projection neurons of the rat spinal cord in response to noxious somatic, articular, and visceral stimulation. *J Comp Neurol*. 1989;285(2):177–195.
61. Renier N, Wu Z, Simon DJ, Yang J, Ariel P, Tessier-Lavigne M. iDISCO: a simple, rapid method to immunolabel large tissue samples for volume imaging. *Cell*. 2014;159(4):896–910.
62. Coggeshall RE. Fos, nociception and the dorsal horn. *Prog Neurobiol*. 2005;77(5):299–352.
63. Todd AJ, Spike RC, Brodbelt AR, Price RF, Shehab SA. Some inhibitory neurons in the spinal cord develop c-fos-immunoreactivity after noxious stimulation. *Neuroscience*. 1994;63(3):805–816.
64. Noguchi K, Kowalski K, Traub R, Solodkin A, Iadarola MJ, Ruda MA. Dynorphin expression and Fos-like immunoreactivity following inflammation induced hyperalgesia are colocalized in spinal cord neurons. *Brain Res Mol Brain Res*. 1991;10(3):227–233.
65. Talbot S, Foster SL, Woolf CJ. Neuroimmunity: Physiology and Pathology. *Annu Rev Immunol*. 2016;34:421–447.
66. Ghasemlou N, Chiu IM, Julien JP, Woolf CJ. CD11b+Ly6G- myeloid cells mediate mechanical inflammatory pain hypersensitivity. *Proc Natl Acad Sci U S A*. 2015;112(49):E6808–E6817.
67. Rocha AC, Fernandes ES, Quintão NL, Campos MM, Calixto JB. Relevance of tumour necrosis factor-alpha for the inflammatory and nociceptive responses evoked by carrageenan in the mouse paw. *Br J Pharmacol*. 2006;148(5):688–695.
68. Cunha FQ, Poole S, Lorenzetti BB, Ferreira SH. The pivotal role of tumour necrosis factor alpha

in the development of inflammatory hyperalgesia. *Br J Pharmacol*. 1992;107(3):660–664.
69. Suter MR, Wen YR, Decosterd I, Ji RR. Do glial cells control pain? *Neuron Glia Biol*. 2007;3(3):255–268.
70. Narita M, et al. Role of interleukin-1beta and tumor necrosis factor-alpha-dependent expression of cyclooxygenase-2 mRNA in thermal hyperalgesia induced by chronic inflammation in mice. *Neuroscience*. 2008;152(2):477–486.
71. Xu ZZ, et al. Resolvins RvE1 and RvD1 attenuate inflammatory pain via central and peripheral actions. *Nat Med*. 2010;16(5):592–597.
72. Lampa J, et al. Peripheral inflammatory disease associated with centrally activated IL-1 system in humans and mice. *Proc Natl Acad Sci U S A*. 2012;109(31):12728–12733.
73. Barde YA, Edgar D, Thoenen H. Purification of a new neurotrophic factor from mammalian brain. *EMBO J*. 1982;1(5):549–553.
74. Thoenen H. Neurotrophins and neuronal plasticity. *Science*. 1995;270(5236):593–598.
75. Michael GJ, et al. Nerve growth factor treatment increases brain-derived neurotrophic factor selectively in TrkA-expressing dorsal root ganglion cells and in their central terminations within the spinal cord. *J Neurosci*. 1997;17(21):8476–8490.
76. Salio C, Averill S, Priestley JV, Merighi A. Costorage of BDNF and neuropeptides within individual dense-core vesicles in central and peripheral neurons. *Dev Neurobiol*. 2007;67(3):326–338.
77. Salio C, Lossi L, Ferrini F, Merighi A. Ultrastructural evidence for a pre- and postsynaptic localization of full-length trkB receptors in substantia gelatinosa (lamina II) of rat and mouse spinal cord. *Eur J Neurosci*. 2005;22(8):1951–1966.
78. Garraway SM, Petruska JC, Mendell LM. BDNF sensitizes the response of lamina II neurons to high threshold primary afferent inputs. *Eur J Neurosci*. 2003;18(9):2467–2476.
79. Thompson SW, Bennett DL, Kerr BJ, Bradbury EJ, McMahon SB. Brain-derived neurotrophic factor is an endogenous modulator of nociceptive responses in the spinal cord. *Proc Natl Acad Sci U S A*. 1999;96(14):7714–7718.
80. Kerr BJ, et al. Brain-derived neurotrophic factor modulates nociceptive sensory inputs and NMDA-evoked responses in the rat spinal cord. *J Neurosci*. 1999;19(12):5138–5148.
81. Groth R, Aanonsen L. Spinal brain-derived neurotrophic factor (BDNF) produces hyperalgesia in normal mice while antisense directed against either BDNF or trkB, prevent inflammation-induced hyperalgesia. *Pain*. 2002;100(1–2):171–181.
82. Taves S, Berta T, Chen G, Ji RR. Microglia and spinal cord synaptic plasticity in persistent pain. *Neural Plast*. 2013;2013:753656.
83. Beggs S, Salter MW. The known knowns of microglia-neuronal signalling in neuropathic pain. *Neurosci Lett*. 2013;557(Pt A):37–42.
84. Ulmann L, et al. Up-regulation of P2X4 receptors in spinal microglia after peripheral nerve injury mediates BDNF release and neuropathic pain. *J Neurosci*. 2008;28(44):11263–11268.
85. Coull JA, et al. BDNF from microglia causes the shift in neuronal anion gradient underlying neuropathic pain. *Nature*. 2005;438(7070):1017–1021.
86. Salio C, Ferrini F. BDNF and GDNF expression in discrete populations of nociceptors. *Ann Anat*. 2016;207:55–61.
87. Lim J, Shoemaker R, Bookbinder L, Anderson D, inventors; Ignyta, Inc, assignee. Diagnosis of rheumatoid arthritis (ra) using differentially methylated loci identified in peripheral blood mononuclear cells, t-cells, b-cells monocytes. US patent WO2014036314A2. August 31, 2012.
88. Hayardeny L, Achiron A, Gurevich M, inventors; Teva Pharmaceutical Industries, Ltd. Teva Pharmaceuticals USA, Inc.Tel Hashomer Medical Research Infrastructure And Services Ltd, assignee. Gene expression biomarkers of laquinimod responsiveness. US patent WO2015038963A1. September 12, 2013.
89. Willis WD, Westlund KN. Neuroanatomy of the pain system and of the pathways that modulate pain. *J Clin Neurophysiol*. 1997;14(1):2–31.
90. Sandkühler J. The organization and function of endogenous antinociceptive systems. *Prog Neurobiol*. 1996;50(1):49–81.
91. Dubner R, Ruda MA. Activity-dependent neuronal plasticity following tissue injury and inflammation. *Trends Neurosci*. 1992;15(3):96–103.
92. Xu XJ, Hökfelt T, Wiesenfeld-Hallin Z. Galanin and spinal pain mechanisms: past, present, and future. *EXS*. 2010;102:39–50.
93. Fayaz A, Croft P, Langford RM, Donaldson LJ, Jones GT. Prevalence of chronic pain in the UK: a systematic review and meta-analysis of population studies. *BMJ Open*. 2016;6(6):e010364.
94. Weisman MH, Witter JP, Reveille JD. The prevalence of inflammatory back pain: population-based estimates from the US National Health and Nutrition Examination Survey, 2009-10. *Ann Rheum Dis*. 2013;72(3):369–373.
95. Hamilton L, Macgregor A, Warmington V, Pinch E, Gaffney K. The prevalence of inflammatory back pain in a UK primary care population. *Rheumatology (Oxford)*. 2014;53(1):161–164.
96. Wall PD, et al. Autotomy following peripheral nerve lesions: experimental anaesthesia dolorosa. *Pain*. 1979;7(2):103–111.
97. Pertin M, Gosselin RD, Decosterd I. The spared nerve injury model of neuropathic pain. *Methods Mol Biol*. 2012;851:205–212.
98. Morris CJ. Carrageenan-induced paw edema in the rat and mouse. *Methods Mol Biol*. 2003;225:115–121.
99. Robinson SP, Langan-Fahey SM, Johnson DA, Jordan VC. Metabolites, pharmacodynamics, and pharmacokinetics of tamoxifen in rats and mice compared with the breast cancer patient. *Drug Metab Dispos*. 1991;19(1):36–43.
100. Bas DB, et al. Collagen antibody-induced arthritis evokes persistent pain with spinal glial involvement and transient prostaglandin dependency. *Arthritis Rheum*. 2012;64(12):3886–3896.
101. Chaplan SR, Bach FW, Pogrel JW, Chung JM, Yaksh TL. Quantitative assessment of tactile allodynia in the rat paw. *J Neurosci Methods*. 1994;53(1):55–63.
102. Peng C, et al. A unilateral negative feedback loop between miR-200 microRNAs and Sox2/E2F3 controls neural progenitor cell-cycle exit and differentiation. *J Neurosci*. 2012;32(38):13292–13308.